Science of the Total Environment 791 (2021) 148270

Contents lists available at ScienceDirect

Science of the Total Environment

journal homepage: www.elsevier.com/locate/scitotenv

A novel granular sludge-based and highly corrosion-resistant bio-concrete in sewers

Yarong Song [a], Kirthi Chetty [b,c], Ulf Garbe [c], Jing Wei [a], Hao Bu [a], Liza O'moore [d], Xuan Li [b], Zhiguo Yuan [a], Timothy McCarthy [b,e], Guangming Jiang [a,b,*]

[a] Advanced Water Management Centre, The University of Queensland, St. Lucia, QLD 4072, Australia
[b] School of Civil, Mining & Environmental Engineering, The University of Wollongong, Wollongong, NSW 2522, Australia
[c] Australian Centre for Neutron Scattering, Australian Nuclear Science and Technology Organization, Lucas Heights, NSW 2234, Australia
[d] School of Civil Engineering, The University of Queensland, St. Lucia, QLD 4072, Australia
[e] Sustainable Buildings Research Centre, University of Wollongong, Wollongong, Australia

HIGHLIGHTS

- A novel design of bio-concrete using wastewater cultivated granular sludge.
- The bio-concrete shows high corrosion resistance in sewer environment.
- SRB in bio-concrete increase concrete surface pH and revert corrosion products.
- Microstructure of corrosion products indicates corrosion development.
- Use of electron and neutron techniques to analyze bio-concrete properties.

GRAPHICAL ABSTRACT

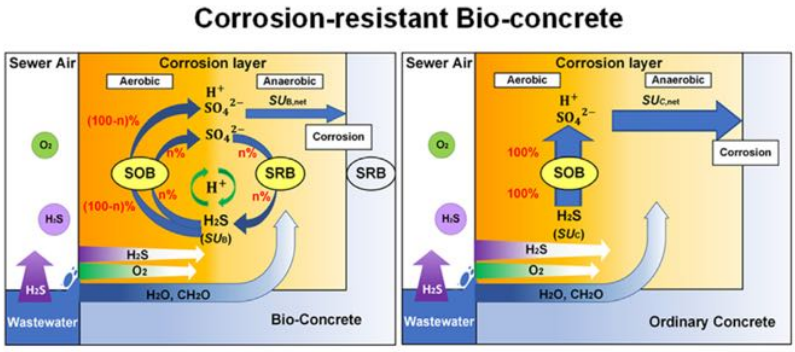

ARTICLE INFO

Article history:
Received 29 April 2021
Received in revised form 27 May 2021
Accepted 30 May 2021
Available online 4 June 2021

Editor: Qilin Wang

Keywords:
Sewer
Bio-concrete
Corrosion
Calcite
Sulfate-reducing bacteria
Nitrate-reducing bacteria

ABSTRACT

Bio-concrete is known for its self-healing capacity although the corrosion resistance was not investigated previously. This study presents an innovative bio-concrete by mixing anaerobic granular sludge into concrete to mitigate sewer corrosion. The control concrete and bio-concrete (with granular sludge at 1% and 2% of the cement weight) were partially submerged in a corrosion chamber for 6 months, simulating the tidal-region corrosion in sewers. The corrosion rates of 1% and 2% bio-concrete were about 17.2% and 42.8% less than that of the control concrete, together with 14.6% and 35.0% less sulfide uptake rates, 15.3% and 55.6% less sulfate concentrations, and higher surface pH (up to 1.8 units). Gypsum and ettringite were major corrosion products but in smaller sizes on bio-concrete than that of control concrete. The total relative abundance of corrosion-causing microorganisms, i.e. sulfide-oxidizing bacteria, was significantly reduced on bio-concrete, while more sulfate-reducing bacteria (SRB) was detected. The corrosion-resistance of bio-concrete was mainly attributed to activities of SRB derived from the granular sludge, which supported the sulfur cycle between the aerobic and anaerobic corrosion sub-layers. This significantly reduced the net production of biogenic sulfuric acid and thus corrosion. The results suggested that the novel granular sludge-based bio-concrete provides a highly potential solution to reduce sewer corrosion.

© 2021 Elsevier B.V. All rights reserved.

1. Introduction

Concrete is the most used material in constructing sewer networks due to its strength and cost-efficiency. Sewer networks are prone to

* Corresponding author at: Advanced Water Management Centre, The University of Queensland, St Lucia, QLD 4072, Australia; School of Civil, Mining and Environmental Engineering, University of Wollongong, Wollongong, NSW 2522, Australia
E-mail address: gjiang@uow.edu.au (G. Jiang).

https://doi.org/10.1016/j.scitotenv.2021.148270
0048-9697/© 2021 Elsevier B.V. All rights reserved.

microbial induced concrete corrosion (MICC) (EPA, 1991; Grengg et al., 2018a), which causes mass loss, cracking and structural collapse (Parker, 1945a; Parker, 1945b; Vollertsen et al., 2008; Joseph et al., 2012). Corrosion of concrete occurs above waterline in gravity sewers. This is mainly caused by hydrogen sulfide (H_2S) generated by anaerobic sulfate-reducing bacteria (SRB) primarily in rising mains (Vahidi et al., 2016; Pikaar et al., 2014). The corrosion development is divided into three sequential stages, i.e. the abiotic pH reduction by CO_2 and H_2S (Stage 1), the biological succession of aerobic sulfide-oxidizing bacteria (SOB) and pH reduction (Stage 2) and active concrete deterioration (Stage 3) (Jahani et al., 2001; Li et al., 2017; Islander et al., 1991; Nielsen et al., 2012). The rehabilitation and replacement of damaged sewers involve an annual cost of around $14 billion in USA and hundreds of millions of dollars in Australia (Boulos and Walker, 2015; Jiang et al., 2015).

To achieve a longer service life, multiple technologies have been developed to alleviate MICC. These technologies include preventing the production and partition of H_2S by chemical dosing in wastewater (Ganigue et al., 2011), and collecting and treating sewer gas enriched in H_2S (Parande et al., 2006; Jiang et al., 2017). To inhibit SOB on concrete surfaces, concrete treatment methods have been practiced, such as applying biocides (e.g. nitrite) (Li et al., 2020a; Sun et al., 2015) or inhibitors (e.g. triclosan) (Negishi et al., 2005; Saraswathy and Song, 2007), elevating surface pH by magnesium hydroxide (Davis et al., 1998) and antimicrobial coatings (e.g. silver-loaded zeolite and polymers) (Haile and Nakhla, 2010; Lebrero et al., 2011; Berndt, 2011; De Muynck et al., 2009). However, these approaches and the production of conventional corrosion-resistant concrete incur substantial costs. Some biocidal coatings and additives are also toxic to environment and humans (Strigul et al., 2010).

Bio-concrete is an innovative type of concrete with admixed bacteria that is capable of microbial induced calcite precipitation (MICP) (Zhu and Dittrich, 2016). Calcite is a 'bio-sealant' to seal cracks and reduce concrete permeability. Urea hydrolysis, denitrification, iron reduction, methane oxidation and sulfate reduction are known microbial activities inducing calcite precipitation (Chahal et al., 2011; Erşan et al., 2015a). For instance, the encapsulated ureolytic nutrients and microorganisms are activated when crack occurs, which produce carbonate to form calcite precipitates in concrete (Da Silva et al., 2015; Achal et al., 2013). However, the high costs involved in the cultivation of axenic cultures and the encapsulation of bacterial spores make the applications difficult (Silva et al., 2015). Also, the ureolytic process can produce large amounts of ammonia, which may induce a secondary pollution for downstream wastewater treatment plants, when such bio-concrete is used in sewers. To date, bio-concrete studies mainly focused on crack-healing of concrete buildings and bridges (Seifan et al., 2016). There remains a need to investigate the application of bio-concrete in sewer environment subject to MICC problems.

A corrosion-resistant bio-concrete to mitigate MICC in sewers requires intrinsic wastewater bacteria that are amenable to non-axenic cultivation, calcite precipitation, self-protection and corrosion resistance, without any secondary pollution. Both nitrate-reducing bacteria (NRB) and SRB exist in wastewater systems due to the prevalence of their substrates in wastewater (Jiang et al., 2009). Denitrifying sludge granules were previously incorporated into concrete as a self-healing additive with $Ca(NO_3)_2$ and $Ca(HCOO)_2$ as nutrients (Erşan et al., 2015b). Another significant pathway for MICP uses SRB in environment enriched in sulfate and calcium ions. SRB can reduce sulfate to sulfide under anaerobic or microaerophilic environment (Okabe et al., 1999; Okabe et al., 2005), generating calcite as well as consuming proton to produce H_2S and CO_2 (Chahal et al., 2011; Satoh et al., 2009). It was found that the spore-forming and haloalkaliphilic SRB were active in alkaline environment with pH up to 11, which is similar to the fresh concrete condition (Hammes and Verstraete, 2002). Furthermore, SOB and SRB were demonstrated to co-exist in the corrosion layer in a sewer manhole, where frequent wastewater inoculation happened (Satoh et al., 2009). Interestingly, less corrosion was detected there compared to the gas-phase samples without wastewater inoculation, suggesting that SRB in the anerobic regions of the corrosion layer may reduce corrosion. It is thus possible to add SRB as the admixture of bio-concrete to mitigate MICC.

This study aims to investigate the effectiveness of a novel type of granular sludge-based bio-concrete to mitigate concrete sewer corrosion. This was produced by mixing a type of self-protected granular sludge enriched with indigenous wastewater bacteria (NRB and SRB) into concrete. The control and bio-concrete mortar coupons (with granular sludge at 1% and 2% of the cement weight) were tested in a laboratory-scale corrosion chamber to simulate sewer corrosive environment (Li et al., 2017; Song et al., 2019a; Jiang et al., 2014a; Cayford et al., 2017; Jiang et al., 2016). The corrosion development were monitored over 6 months using well-established methods including surface pH, sulfide uptake rate, sulfate, corrosion rate, microbial community and a set of advanced electron and neutron analyses. The results provide a detailed evaluation of the corrosion-resistance, indicating a significant breakthrough in using bio-concrete in sewers.

2. Materials and methods

2.1. Granular sludge cultivation

A lab-scale upflow anaerobic sludge blanket (UASB) reactor, filled with synthetic wastewater (Section S1.1, Table S1.1) under anaerobic conditions, was set up to cultivate self-protected granular sludge enriched with NRB and SRB. The compact form and the layered structure of granular biomass is advantageous for protection of the bacteria at the core. The use of a protective carrier (encapsulation) is thus avoided. The reactor was made of Perspex™, with a volume of 4 L, a diameter of 80 mm and a height of 800 mm (Fig. S1.1). The UASB reactor was operated at 23–25 °C, and the pH was controlled at around 7 by a programmable logic controller (PLC) through dosing HCl (10%) and $Na_2CO_3 \cdot 10H_2O$ (28.62 g/L) buffer solutions. To ensure the anaerobic or anoxic condition, the oxidation-reduction potential (ORP) was monitored continuously (around −200 mV). The up-flow velocity was controlled at 1.2 m/h by recirculating the synthetic wastewater at a rate 8 times of the influent flowrate, with 6 h as the hydraulic retention time (HRT). Besides, H_2O_2 (30%) and NaOH solutions (40 g/L) were used to treat the effluent and biogas generated in the reactor before they were discharged.

Anaerobic granules from a local brewery wastewater treatment plant (Brisbane, Australia) were inoculated into the UASB reactor after being sieved (200 μm) for 3 times with a weight of around 1000 g (wet weight). The granules cultivation with SRB and NRB was conducted in two steps (Step I and II, Section S1.2). In Step I, SRB was enriched and granulated in 2 stages: methanogens inhibition (Stage 1, 30% sulfate removal) and SRB enrichment (Stage 2, 50% sulfate removal). Similar processes were conducted to cultivate NRB in the outer layer of the granules in Step II (80% nitrate removal) (Fig. S1.2). The UASB reactor was operated for 14 months (9 months for Step I, 5 months for Step II) to reach stable performances indicated by 50% sulfate and 80% nitrate removals before extracting the granules for bio-concrete production. The extracted granules were prepared as reported, i.e. dried in an oven (Thermotec 2000, Contherm) at 60 °C for 2 days before being mixed in concrete (Erşan et al., 2015a).

2.2. Bio-concrete coupon preparation and characterisation

The mortar mix (Table S2.1) for the coupons was based on the AS 3972 (AS3972, 2010), using ordinary Portland cement (OPC, Cement Australia Builders Cement, Section S2.1 and Table S2.2). To determine the effectiveness of the bio-concrete within a reasonable timeframe, coarse aggregates were avoided while coarse and fine sands were added (Satoh et al., 2009). The water/cement mass ratio was fixed at

0.5 (Erşan et al., 2015a; Erşan et al., 2016). For bio-concrete mortars, sludge granules (Fig. S2.1) were added to achieve levels at 1% and 2% of the cement by weight. $Ca(NO_3)_2$ was added in the bio-concrete to achieve 3% of the cement by weight, for the activity of NRB. Sulfate needed for SRB would be generated in-situ once concrete corrosion occurs (Song et al., 2019a; Hvitved-Jacobsen et al., 2013). No extra organics were added to concrete as sufficient organic matters are available in sewage for both NRB and SRB (Zhu and Dittrich, 2016).

Both the control and bio-concrete mortar coupons were cast in dimensions of 80 mm (length) × 40 mm (width) × 40 mm (depth). After casting, the coupons were cured in moist air for 24 h and then in lime-saturated water for 28 days (Li et al., 2020a). After retrieval from the curing tank, the coupons were dried in room temperature (30 °C) for 2 weeks to achieve a similar and stable initial water content (Wang et al., 2012a). Two coupons were then embedded as a pair (duplicates) using epoxy resin (FGI R180 epoxy and H180 hardener) in a stainless steel frame, with one surface (80 mm (length) × 40 mm (width)) exposed as the tested surface (Jiang et al., 2015; Jiang et al., 2014a). The Stainless steel frame provides a reference point to determine the coupon thickness loss due to corrosion (Section 2.4) (Jiang et al., 2014a).

Mechanical properties including the compressive strength and porosity were measured to ensure that the control and bio-concrete mortars meet the requirements of sewer pipes. The compressive strength was tested in accordance with the AS 1012.9 (Section S2.2, Table S2.3) (AS1012.9, 2014). Determination of the apparent volume of permeable voids (AVPV) was carried out according to AS 1012.21 (Section S2.3, Table S2.4) (AS1012.21, 1999). The volume and distribution of the granular sludge in the bio-concrete was investigated using Neutron Tomography (DINGO) at the Australian Nuclear Science and Technology Organization (ANSTO) (Garbe et al., 2015; Oromiehie et al., 2020). The principle and operational parameters were elucidated in Section S2.4.

2.3. Corrosion chamber and exposure conditions

A corrosion chamber (Fig. S3.1) was built to achieve a controlled environment simulating real sewer conditions (Jiang et al., 2015; Jiang et al., 2014a; Song et al., 2019b). It was constructed of 51 mm thick PVC panels, with the dimension of 1436 mm (length) × 1155 mm (width) × 1475 mm (height). 50 L of real domestic wastewater (collected from a local sewer pumping station and replaced monthly) was continuously recirculated in the chamber (wastewater properties in Table S3.1, S3.2).

The chamber operation state was manipulated using Lab-View (Lab-View, 2014; Real Time). The gaseous H_2S concentration was controlled at 50 ppm in the corrosion chamber by PLC (Section S3.1). The air temperature and relative humidity were monitored using the handheld humidity meter (HM70, Vaisala, Finland) weekly. To avoid wastewater acidification due to absorption of H_2S, the wastewater pH was automatically controlled at around 7.5 by dosing alkaline (NaOH, 40 g/L, Section S3.2). The wastewater temperature was maintained at about 27–29 °C by heating the wastewater in the sewage tank and recirculating the heated wastewater back to the chamber. During the 6-month coupon exposure, the gaseous H_2S level, wastewater pH and temperature in the corrosion chamber were controlled at 50 ± 5 ppm, 7.5 ± 0.5, and 28 ± 0.5 °C (Fig. S3.2). The relative humidity was 90–95% and the air temperature at 23–25 °C. This simulated a typical sewer condition favourable for corrosion investigation (Jiang et al., 2014a; Jiang et al., 2016; Song et al., 2019b; Wells and Melchers, 2014).

In this study, six coupon pairs, i.e. two control pairs (C0-a and C0-b), two 1% bio-concrete pairs (B1-a and B1-b) and two 2% bio-concrete pairs (B2-a and B2-b) were partially submerged (approx. 20 mm) in the wastewater. As demonstrated previously, this arrangement well simulated the position of tidal region in sewers, a location highly susceptible to MICC due to wastewater inoculation and nutrients availability for specific heterotrophic microorganisms (Li et al., 2017; Jiang et al., 2015; Song et al., 2019a; Jiang et al., 2014a).

2.4. Corrosion sampling and analysis

The partially submerged coupon surfaces were utilized for corrosion sampling and analysis. They were exposed in the corrosion chamber for 6 months, during which they were retrieved monthly for corrosion morphology inspection and surface pH measurement using a flat surface-pH electrode (Extech PH150-C concrete pH kit, Extech Instruments) (Song et al., 2020). After 6 months, C0-a, B1-a and B2-a were tested for sulfide uptake rate (SUR); then they were destructively sampled for physico-chemical and microbial analysis, and C0-b, B1-b and B2-b for mineral liberation analysis (MLA).

Coupons were placed into a sealed reactor with 100% relative humidity to test the SUR (Sun et al., 2014). H_2S gas was generated and injected into the reactor to achieve a gaseous concentration of around 60 ppm. The H_2S concentration in the reactor was then monitored continuously using a H_2S detector (App-Tek OdaLog Logger L2, the detection range of 0–200 ppm) until the gaseous H_2S concentration dropped to around 40 ppm (Li et al., 2020a; Jiang et al., 2016). This concentration range was based on the average H_2S concentrations achieved in the chamber. The SUR was determined by calculating the slope of the measured H_2S concentration versus time. Thus, the average SUR of the coupons at 50 ppm was calculated from 3 to 4 replicate measurements.

Sulfur species and their concentrations on the corroded concrete surface were determined by sampling the corrosion products of a known surface area at three independent locations of each coupon (Li et al., 2020a). The corrosion products were dispersed into sulfide antioxidant buffer solution and measured using ion chromatography (Dionex ICS-2000) for dissolved inorganic sulfur compounds (Jiang et al., 2015; Song et al., 2019a). Afterwards, the rest of corrosion products were completely removed with a sterile scalpel directly into 50 mL falcon tubes. One third of the corrosion products were used for analysis of micro-level corrosion morphology and element compositions using Field Emission Scanning Electron Microscope (FE-SEM) and Energy Dispersive X-ray Spectroscopy (EDS), while the remaining corrosion products were used for microbial community analysis.

After the corrosion layer removal, the coupons were further washed with high pressure washer (Karcher K 5.20 M). The corrosion loss of each coupon was determined by the photogrammetry methodology to compare the surface average thickness before and after corrosion. (Jiang et al., 2014a; Wells and Melchers, 2015; Wells et al., 2009) The details of the photogrammetry methodology were delineated in Section S4.1.

2.5. SEM, EDS and MLA

The corrosion products were identified by FE-SEM (JEOL JSM-7001F, America) equipped with a detector (Oxford 50 mm2 X-Max SDD x-ray) that enabled simultaneous imaging and element analysis (EDAX, AMETEK Inc) at high count rates with 125 eV energy resolutions. The spot locations for element analysis were chosen by examining the Backscattered Electron Image (BSE) (Zhao et al., 2012; Fandrich et al., 2007). Prior to the test, the corrosion products were vacuum dried at 70 °C for 7 h (SEMSA OVEN 718), coated with 30–40 nm thick carbon (Quorum Q150T, UK) and plasma cleaned (Evactron 25 Plasma Cleaner) (Lai et al., 2018a).

The amount, nature and distribution of minerals (the corroded and intact concrete) were identified by MLA (Section S4.2) (Song et al., 2020; Jiang et al., 2014b; Sun et al., 2016). The coupon pairs untouched by the destructive sampling were sliced into around 10 mm-thick cross-sections by cutting the coupons perpendicularly to the long side of the coupon frame. The sections were then casted by low-viscosity epoxy resin to minimize any artificial damage before being further trimmed into smaller sections (20 mm (length) × 20 mm (width) × 10 mm

(thickness)) to keep the corrosion layer as well as the adjacent intact concrete. Prior to MLA, the sections were ground, polished and coated with carbon approximately 25 nm thick (JEOL JEE-420 vacuum evaporator).

2.6. Microbial community analysis

The corrosion products sampled for microbial analysis were stored at 4 °C for <24 h prior to the cell extraction (Jiang et al., 2016; Cayford et al., 2012). In brief, the cell extraction procedure includes sonication to loosen the cells from the corrosion products, concentrating the cells from a sucrose gradient, and then washing and centrifuging the cells gradually. The FastDNA™ SPIN Kit for Soil (MP Biomedicals, CA) was used to extract DNA from the separated cells following the manufacture's protocol. To perform 16S rRNA gene amplicon sequencing, the extracted DNA samples were sent to the Australia Centre for Ecogenomics (Brisbane, Australia). PCR amplifications were conducted by using the universal primers 926F (5'-AAACTYAAAKGAATTGRCGG-3′) and 1392R (5'-ACGGGCGGTGWGTRC-3′). Barcoded library construction and paired-end sequencing were performed on a MiSeq Sequencing System (Illumina). The detailed processing of the sequencing data and community analysis were specified in Section S4.3.

3. Results and discussion

3.1. Bio-concrete characterisation and mechanical properties

For most of the sewer concrete, 50 MPa is the minimum 28-day compressive strength requirement (AS1012.9, 2014; Li et al., 2020b) and this was achieved by all control and bio-concrete mortal coupons (Table S2.3). Due to the admixture of granular sludges as organic matters, the compressive strength of B1 and B2 decreased slightly by around 1.2% and 3.3% compared to that of C0. Similar adverse impacts of organic matters on the compressive strength of cement-based composites were reported previously, likely attributed to the organic effects on cement hydration and pozzolanic reaction (Ma et al., 2016). In addition, a concrete with AVPV values <13% is usually classified as good-quality concrete for bridges and roads (Li et al., 2020b), although no specific AVPV is required for sewer-related infrastructures. The AVPV of both control and bio-concrete met this general limit, while it increased from 10.9 ± 1.1% in C0 to 12.7 ± 0.9% and 13.0 ± 0.1% in B1 and B2 (Table S2.4). The AVPV values were in the similar ranges of cement mortar and OPC concrete (Chen et al., 2013). Although slightly reduced compressive strength and increased porosity were observed for the bio-concrete, the statistics analysis indicated that their differences between control and bio-concrete were insignificant ($p > 0.05$).

The distribution and volume of granular sludge in the bio-concrete were characterized by neutron tomography (Fig. 1). No organic granules were observed in control coupon. The total volume ratios of granular sludge inside the coupons for B1 and B2 were around 0.74% and 1.56% (1:2), consistent with the weight ratio (1:2) of granular sludge added. Moreover, the granule volumes were not uniform inside each coupon type, reaching up to 12.2 mm^3 in B1 and 28.0 mm^3 in B2. The smaller granules in B1 than B2 was likely due to the dispersion and break-down of some granules during the cement mixing process. Overall, the results demonstrated that the sludge granules were evenly distributed in the bio-concrete.

3.2. Corrosion development on bio-concrete

The visual inspections demonstrated that all concrete coupons developed corrosion gradually (Fig. 2a). After 3 months of exposure, an evident wastewater level was observed with different surface morphologies between regions above and below (Song et al., 2019a). Some white or yellowish, relatively dry corrosion products were seen above the wastewater level, as typical characteristics of tidal regions (Li et al., 2017; Song et al., 2019a; Jiang et al., 2016). As the exposure increased, the corrosion products grew much thicker and more moisturized on C0, while less corrosion was observed on B1 and the least corrosion on B2.

Surface pH is a good indicator of corrosion development due to continuous acidification by MICC and subsequent neutralization of cementitious compounds (Li et al., 2020a). The initial pH values of all coupons were around 10 prior to the exposure (Fig. 2b). This was close to the carbonate-bicarbonate equilibrium ($pK_a = 10.3$) that indicated the carbonation during manufacture or storage of the coupons (Islander et al., 1991; Koch et al., 2002). The surface pH decreased clearly with time, suggesting the continuous acid production. Although the decreasing trend was observed for all coupons, higher pH values were evident on the bio-concrete (pH 4–5) compared to the control concrete (around pH 3). The relatively low pH on C0 indicated the active corrosion (Stage 3), while B1 and B2 were at Stage 2 according to the 3-stage theory (Jiang et al., 2015; Okabe et al., 2005). In particular, the pH differences between C0 and B1, C0 and B2, and B1 and B2 became highly significant ($p < 0.01$) after 4 months, suggesting a reduced acidification of the bio-concrete.

SUR represents the sulfide-oxidizing activity on the concrete surface, which is commonly used to evaluate the sulfide uptake capability of the corrosion biofilm (Sun et al., 2014). After 6 months of exposure, the SUR of all coupons reached to 100–160 $mgS/m^2 \cdot h$ (Fig. 2c), suggesting the active sulfide uptake on both control and bio-concrete. However, around 14.6% and 35.0% SUR reductions were observed on B1 and B2 compared to C0, indicating that SOB activities and sulfide uptake were less on the bio-concrete surfaces after 6 months. Significant SUR differences were observed between B2 and C0, and B2 and B1 ($P < 0.05$).

Once H_2S is consumed by SOB, sulfate and proton produced can be used to quantitatively compare the ultimate sulfuric acid generation that causes corrosion. The sulfate content of C0 and B1 reached to 70–90 gS/m^2 (Fig. 2c), similar to that detected after 12 months of exposure in a real sewer manhole with 20–40 ppm of H_2S (Li et al., 2020a). Comparably, much lower sulfate was observed for B2 (39.4 ± 6.8 gS/m^2). The sulfate levels of B1 and B2 were 15.3% and 55.6% less

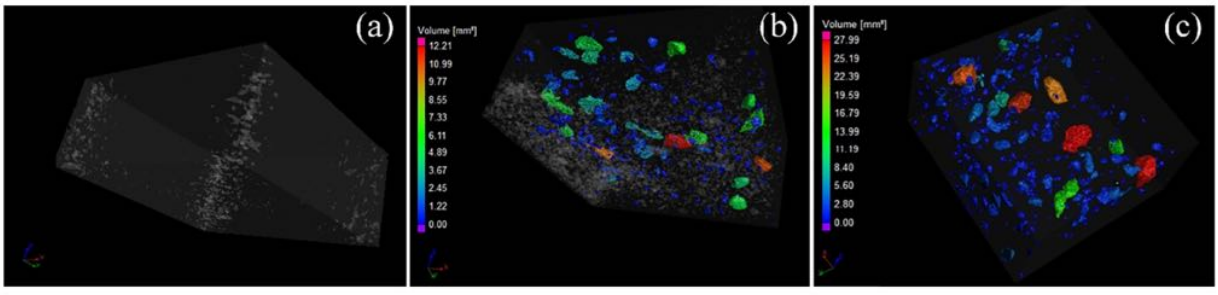

Fig. 1. The volume and distribution of granular sludge in control coupon-C0 (a), bio-concrete-B1 (b) and B2 (c). The coloured areas represented the sludge granules, with the color-coding assigned to the granular sizes indicated in the legend.

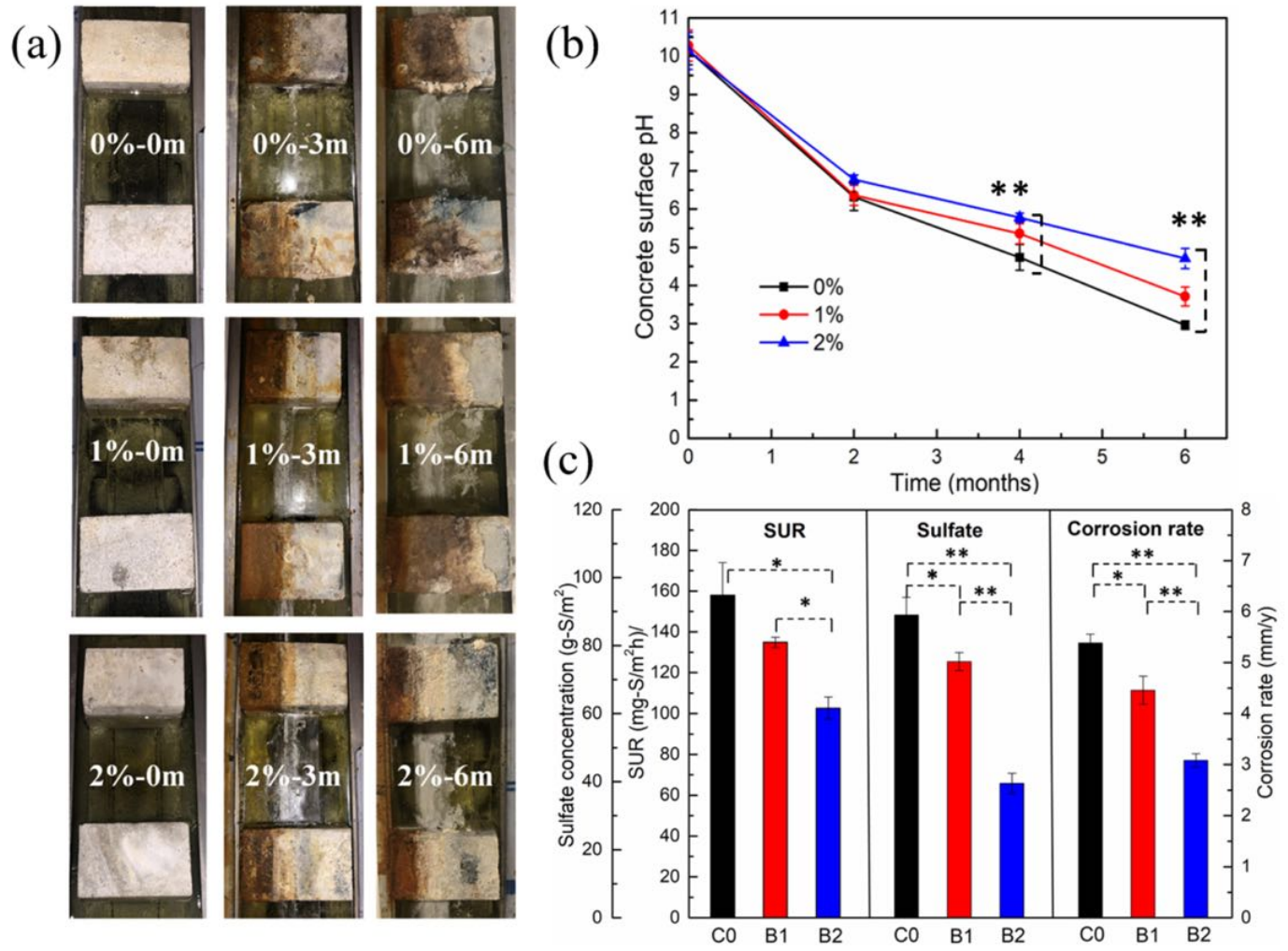

Fig. 2. Visual inspection of control (C0) and bio-concrete mortar coupons (B1 and B2) after 0, 3 and 6 months of partially submerged exposure in the corrosion chamber (a); their pH profiles during the 6-month exposure (b); the sulfide uptake rates (SUR), sulfate concentrations and corrosion rates after 6 months of exposure (c). The error bars indicated the standard errors. Single-factor ANOVA analysis was used to calculate the significant difference among the groups (** indicated highly significant difference, $p < 0.01$; * indicated significant difference, $p < 0.05$).

than that of C0, with significant difference detected between C0 and B1 ($p < 0.05$), and highly significant differences between B2 and C0, and B2 and B1 ($p < 0.01$). Interestingly, the reduction ratios of the ultimate sulfate production that causes corrosion were higher than the reductions of biological sulfide uptake, indicating that the sulfide uptake by bio-concrete was not completely used to cause corrosion (detailed discussion in Section 3.5).

The MICC development eventually caused the mass loss of concrete coupons (Fig. 2c). It was found that the corrosion rates decreased in the order of C0 > B1 > B2. The results were comparable to previously reported corrosion rates in laboratory and field studies (Grengg et al., 2018a; Jiang et al., 2016; Wells and Melchers, 2015). C0 showed significantly higher ($p < 0.05$) corrosion rates than B1, while highly significant difference ($p < 0.01$) was detected between C0 and B2, and B1 and B2. The corrosion rates of B1 and B2 were about 17.2% and 42.8% less than that of C0. Overall, the results above strongly indicated that the granular sludge-based bio-concrete (B2 and B1) were more corrosion-resistant than the general concrete (C0).

3.3. Characterisation of corrosion products

It is essential to understand the different corrosion resistance of bio-concrete and control coupons by characterizing the corrosion products, i.e. microstructure and element compositions (Grengg et al., 2018b; Grengg et al., 2020). The results (Fig. 3) showed that crystals formed on all types of coupons were similar in shape, i.e. typically flake-like parallelogram or hexagon, which is the classic morphology of gypsum ($CaSO_4$) (Song et al., 2019a; Choi et al., 2018). This was verified by EDS, which showed Ca, S and O as major element compositions (Fig. S4.1). Gypsum was thus likely one of the major corrosion products, the typical feature of MICC, for both control and bio-concrete (Li et al., 2017; Cayford et al., 2017; Jiang et al., 2014b).

Evident differences in crystal sizes of gypsum were observed among C0, B1 and B2. The dimensions of the gypsum crystal was evaluated in two directions, namely 'length' and 'width' (Choi et al., 2018). For C0, the crystal length was in the range of 0.2–3 μm and width of 0.3–2 μm (Fig. 3b). Comparably, evidently larger crystals were observed on B1 and B2 (Fig. 3d and f), with length in the range of 0.3–8 μm and width of 0.2–5 μm. It was suggested that the gypsum crystal size can be greatly influenced by pH levels, i.e., higher pH increases the size (Choi et al., 2018). In such, the smaller crystal size on C0 was corresponded with the lower pH value, while larger sizes on B1 and B2 were attributed to higher pH values (Fig. 2b). Additionally, the potential existence of some extracellular polymeric substances (EPS) (Lai et al., 2018b) were observed among the crystalline corrosion products (rectangular areas in Fig. 3). More EPS were identified in C0 compared to that of B1 and

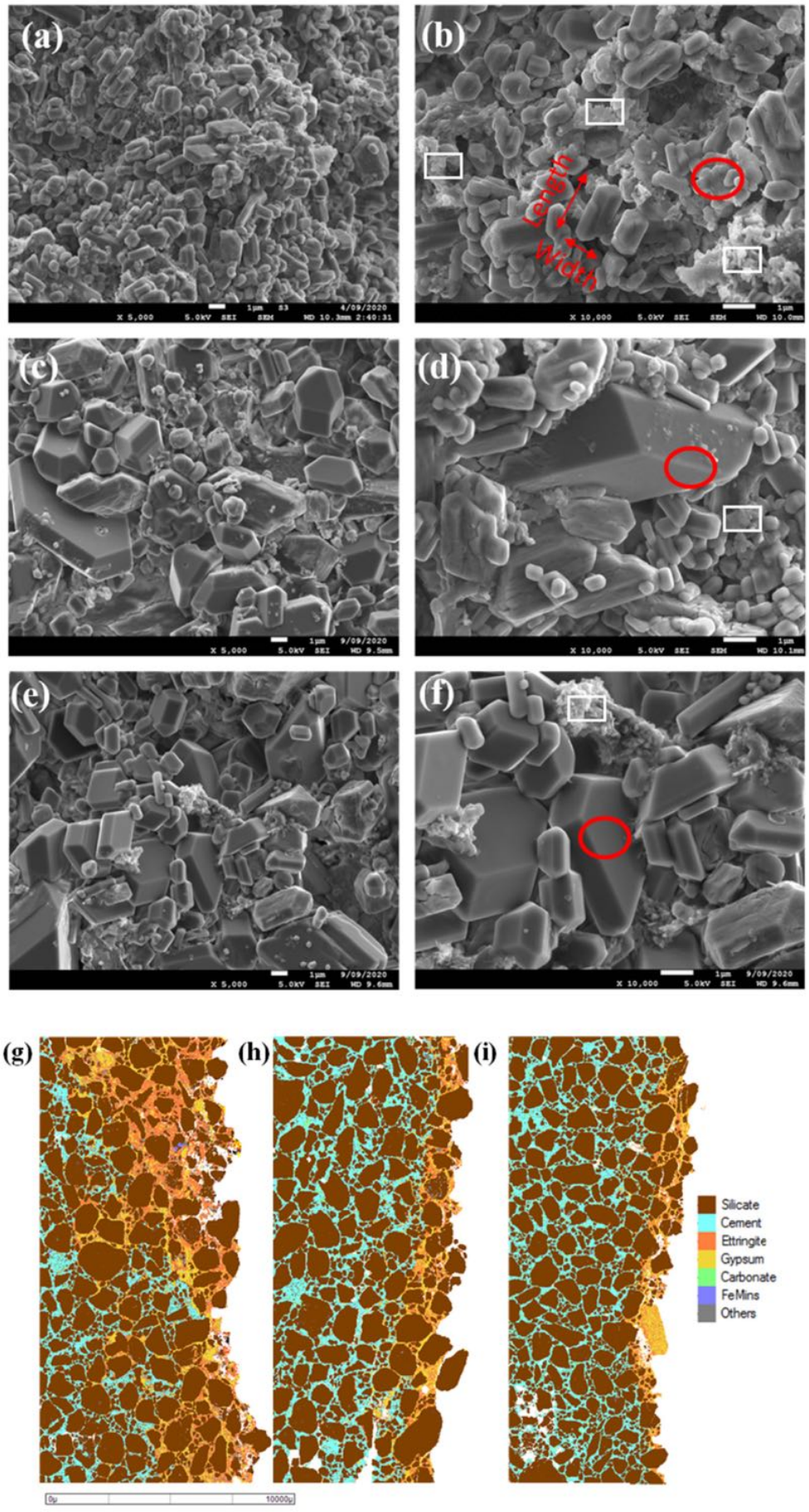
(a)
(b)
Length
Width
(c)
(d)
(e)
(f)
(g)
(h)
(i)
Silicate
Cement
Ettringite
Gypsum
Carbonate
FeMins
Others

B2, which likely suggested more biomass on the corrosion layer of control coupons.

As SEM and EDS analysis only showed the microstructure and element compositions of corrosion products, the mineral distribution and composition were further investigated using MLA, an efficient tool to determine the mineral depth profile (Song et al., 2020). MLA clearly visualized a much thicker corrosion layer on C0 compared to B1 and B2 (Fig. 3g-i). The results confirmed that gypsum was one of the predominant corrosion products. Ettringite was also observed, which was well recognized as another significant corrosion products (Parande et al., 2006; Song et al., 2020; Monteny et al., 2000). As suggested previously, gypsum prefers to be formed near the surface of corrosion layers while ettringite tends to grow near the intact concrete, depending on the sulfate concentrations, cement type and pH depth profile (Jiang et al., 2014b; Mori et al., 1992). Similarly, ettringite was preferentially formed adjacent to the intact concrete, especially for B1 (Fig. 3h) and B2 (Fig. 3i), although no evident boundary was observed between the two corrosion products. The inconspicuous boundary might be due to the falling-off of the loose outer corrosion layer composed of mainly gypsum (0.5-2 mm) during the preparation for MLA, as evidenced by the sinking curve of the corrosion layer on C0 (Fig. 3g).

3.4. Microbial community analysis

The rarefaction curves of all 6 samples reached asymptotic states, indicating that the sequencing covered the majority of microbial diversity (Fig. S4.2). Species richness (Chao) and diversity (Shannon and Simpson indexes) of all coupons, within the similar range compared to those reported previously (Li et al., 2020a; Song et al., 2019a), suggested a well simulation of real sewer corrosion (Table S4.1). Examination of the rarefaction (Fig. S4.2) and rank abundance (Fig. S4.3) showed that the community diversity decreased in the order of C0 > B1 > B2, which might be related with the various surface pH (Fig. 2b). It was reported that sewer concrete pH increased with depth (Jiang et al., 2014b). Therefore, a lower surface pH on C0 would lead to a wider pH range from the surface (around pH 2.9) to the intact concrete (higher than 11), which were suitable for a more diverse bacterial proliferation. Comparably, the relatively high pH level on B2 (around pH 4.7) may inhibit the microbial diversity due to the narrower pH range.

The heatmap representing the relative abundance of predominant bacterial types (>2% in at least one sample) at the genus level in the corrosion samples was presented (Fig. 4). A great amount of acidophilic SOB, mainly *Acidithiobacillus, Sulfobacillus* and *Thiomonas* were observed in the microbial communities after 6 months of exposure. The most abundant *Acidithiobacillus* were continuously reported as the typical genus of autotrophic SOB, detected by both culture dependent and independent methods (Parker, 1945a; Li et al., 2017; Islander et al., 1991; Okabe et al., 2007). *Sulfobacillus* and *Thiomonas* were also known for their ability to oxidize reduced sulfur to sulfate in laboratory corrosion chambers (Jiang et al., 2016), real sewers (Cayford et al., 2017; Cayford et al., 2012) as well as wastewater treatment utilities (Ling et al., 2014).

Except for the conventional SOB, other heterotrophic acidophiles were also identified (Li et al., 2017). Particularly, *Ferroplasma* and *Mycobacterium* were found to comprise a great proportion of the communities. *Ferroplasma* was previously observed in acidic corroded concrete biofilms in real sewers (Li et al., 2020a; Ling, 2013). They were commonly recognized for their iron-oxidizing capabilities in ore and mining industry (Dopson et al., 2004). A recent study on acid mine drainage treatment speculated that some of the *Ferroplasma*-like populations may metabolize intermediate inorganic sulfur compounds by multiple pathways thus producing sulfuric acid (Ni et al., 2018). However, the sulfur-oxidation capabilities have not been confirmed. Similar research questions remain to be addressed for Mycobacterium, that were often abundant in acidophilic communities of sewer corrosion layers, especially at the tidal regions (Li et al., 2020a; Song et al., 2019a; Cayford et al., 2017; Jiang et al., 2016). They can scavenge organics which are favourable for the growth of autotrophic SOB, whereas the capabilities to oxidize sulfur and induce corrosion have not been confirmed. Evident decrease of *Ferroplasma* and increase of *Mycobacterium* were observed in B2, of which further study is needed to investigate their potential functions in the bio-concrete corrosion. More intriguingly, a typical genus of SRB, i.e. *Desulfobacter*, was detected in both corrosion products of B1 and B2, while they were not observed on C0 nor in wastewater used. Therefore, the SRB should be derived from the granular sludge admixed into the concrete, which accounted for the 50% sulfate removal rate during the sludge cultivation (Section S1.2). *Desulfobacter* was previously reported as one of the representative sulfate-reducing anaerobes found in the deposition layers on the bottom of real sewer pipes or coupon surface (Li et al., 2017; Song et al., 2019a; Cayford et al., 2017). Another study successfully visualized a significant amount of *Desulfobacterales* which were coexisting with SOB in the corrosion layer of a real sewer manhole, by using fluorescent in situ hybridization (Satoh et al., 2009).

Overall, the clustering and relatedness analysis showed that the microbial community structures of C0, B1 and B2 were evidently separated (Fig. S4.4). This might be attributed to the different bacterial diversity (Fig. S4.2, S4.3) and the variations in the abundance of key SOB (*Acidithiobacillus, Sulfobacillus* and *Thiomonas*) as well as SRB (*Desulfobacter*). The statistics analysis presented that the total abundance of SOB decreased highly significantly from C0 (56.08 ± 4.62%) to B1 (33.66 ± 1.25%) and B2 (16.43 ± 1.79%) ($p < 0.01$); while the abundance of SRB increased highly significantly from C0 (none) to B1 (2.05 ± 0.07%) and B2 (6.81 ± 0.27%) ($p < 0.01$). The relatively low ratios of SRB was probably due to:1) the highly diverse community in the corrosion layer (Grengg et al., 2018a; Li et al., 2020a); 2) their limited viability requiring anaerobic conditions; 3) the transport limitations of sulfate and organic compounds into the anaerobic region away from the surface layer. However, as demonstrated previously, the SRB with relative abundance even lower than 1% in the corrosion layer successfully inhibited corrosion compared to those samples without SRB (Satoh et al., 2009).

3.5. A conceptual model of corrosion-resistant bio-concrete

The analysis of physicochemical characteristics, compositions and distribution of corrosion products as well as microbial communities consistently demonstrated that the bio-concrete coupons were more corrosion-resistant than the control coupons. This was unlikely caused by the mechanical and structural concrete properties, because no significant difference was detected in the compressive strength and porosity between bio-concrete and control coupons. The slightly increased AVPV of B1 and B2 compared to C0 may even accelerate corrosion due to easier accesses of H_2S, sulfate, acid and other corrosive substances (Li et al., 2020b). Instead, the increased pH, the reduced sulfide uptake and ultimate sulfate production indicated that the enhanced corrosion-resistance of bio-concrete should be mainly attributed to the altered microbial activities of SOB and SRB.

Concrete sewer corrosion mainly occurs on concrete surface where H_2S and O_2 are available. However, the concentrations of O_2 and H_2S decrease drastically to zero within the uppermost 400 μm of the biofilm due to biochemical process and diffusion limitation (Satoh et al., 2009). The corrosion layer, with a few thousand μm thickness (Okabe et al., 2007), can be divided into aerobic and anaerobic layers (Fig. 5).

Fig. 3. SEM images of concrete corrosion products on the surface of C0 (a, ×5000; b, ×10,000), B1 (c, ×5000; d, ×10,000) and B2 (e, ×5000; f, ×10,000), and MLA mapping of primary mineral components on the cross-sections of C0 (g), B1 (h) and B2 (i) after 6 months of partially submerged exposure in the corrosion chamber. The corresponding element compositions of the circled area were shown in Fig. S4.1. Presence of EPS was indicated in the rectangular areas.

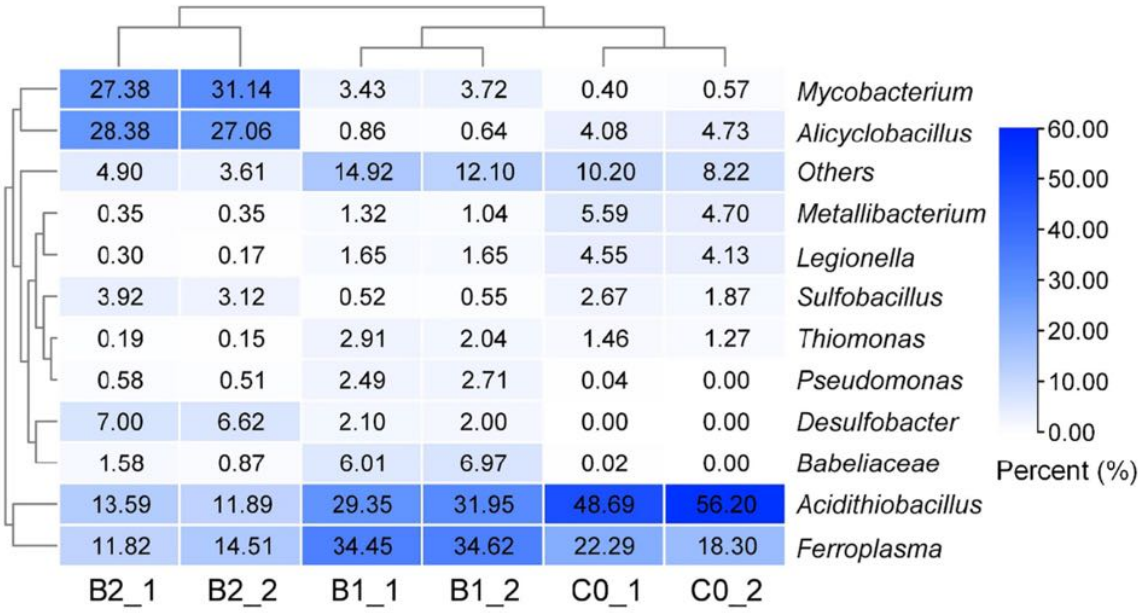

Fig. 4. Heatmap representing the relative abundance of the predominant bacterial types (>2% in at least one sample) at the genus level detected in the corrosion layer of C0, B1 and B2 after 6 months of partially-submerged exposure in the corrosion chamber. Two samples were obtained from each type as duplicates.

In the aerobic layer, the diffusion of H_2S and O_2 is crucial for SOB activities (e.g. *Acidithiobacillus, Sulfobacillus* and *Thiomonas*), which produces abundant sulfate and proton. The sulfate and proton, together with organic compounds in wastewater (VFAs, sugar and proteins etc.) and volatile organics in sewer atmosphere, diffuse into the anaerobic region to nurture SRB (e.g. *Desulfobacter*) (Li et al., 2017; Wang et al., 2012b). Then the SRB activities consume sulfate and proton to increase pH and produce H_2S. This agrees with a previous study that observed enhanced pH and H_2S levels due to SRB activities in the anaerobic concrete corrosion layer in a sewer manhole (Satoh et al., 2009). The SRB activities also produce CO_2 (Eqs. (1)–(2)) and possibly convert the corrosion products (gypsum) to calcite (Eq. (3)), depending on the ionization equilibrium of the carbonic acid (Dickson and Millero, 1987). In the acidic corrosion layers (pH < 4), CO_2 is more likely produced (Eq. (2)) (Satoh et al., 2009; Jiang et al., 2014b), whereas calcite would be generated if bicarbonate is present at higher pH range of 4–7 (Eqs. (1) and (3)).

$$2CH_2O + SO_4^{2-} + H^+ \rightarrow H_2S + HCO_3^- + CO_2 + H_2O \quad (1)$$

$$2CH_2O + SO_4^{2-} + 2H^+ \rightarrow H_2S + 2CO_2 + 2H_2O \ (pH<4) \quad (2)$$

$$2HCO_3^- + Ca^{2+} \rightarrow H_2O + CaCO_3 + CO_2 + H_2O \ (pH = 4-7) \quad (3)$$

The H_2S produced in the anaerobic layer then diffuse back into the aerobic corrosion layer, where it is further oxidized by SOB. Accordingly, a sulfur and proton cycle between the two layers forms. For bio-concrete, the sulfur cycle keeps a portion (n%) of the biological sulfide uptake (SU_B) in the loop, while the rest ((100−n) %) of SU_B is ultimately transformed to net sulfuric acid ($SU_{B,\,net}$) that leads to reduced corrosion on the bio-concrete (Eq. (4)). Comparably, for control concrete, 100% of the biological sulfide uptake (SU_C) is transformed to net sulfuric acid ($SU_{C,\,net}$, Eq. (5)) (Li et al., 2017). Meanwhile, the reduced net acid production that leads to a higher pH (1.8 unit) on bio-concrete further restrains the proliferation of acidophilic SOB, which in turn reduces SU_B compared to SU_C. Therefore, $SU_{B,\,net}$ is evidently reduced in comparison with $SU_{C,\,net}$, due to the less biological sulfide uptake and the sulfur cycle.

$$SU_{B,net} = SU_B \times (100-n)\% \quad (4)$$

$$SU_{C,net} = SU_C \times 100\% \quad (5)$$

The reduced SU_B compared to SU_C was supported by 14.6% and 35.0% SUR reduction of B1 and B2 compared to C0. Besides, the higher reduction ratios of $SU_{B,\,net}$ compared to $SU_{C,\,net}$, evidenced by 15.3% and 55.6% less sulfate detected on B1 and B2 compared to C0, demonstrated the sulfur cycle that further reduced the bio-concrete corrosion. Future studies need to quantitatively characterize the dynamics of SOB and SRB in the bio-concrete sulfur cycle to determine the sulfur cycling percentage (n%). To enhance the corrosion resistance, more research is needed to reduce $SU_{B,\,net}$ by increasing the activity and abundance of SRB in the corrosion layer.

In comparison to the evident colonization of SRB, no NRB was detected after 6 months. NRB can consume proton, increase concrete pH (Eq. (6)) and produce calcite (Eq. (7)) (Erşan et al., 2015a; Erşan et al., 2016). The 80% nitrate removal rate during the sludge cultivation demonstrated that NRB grew successfully in the sludge (Section S1.2). The absence of NRB was likely due to the depletion of nitrate by 6 months of exposure (no nitrate was detected in the corrosion layer). In comparison, because of the continuous generation of sulfate by MICC, SRB became dominated in the anerobic layer. Further investigations to elucidate the NRB activity at different corrosion stages are necessary in future.

$$5CH_2O + 4NO_3^- + 4H^+ \rightarrow 2N_2 + 5CO_2 + 7H_2O \quad (6)$$

$$Ca^{2+} + CO_2 + 2OH^- \rightarrow CaCO_3 + H_2O \quad (7)$$

Overall, this study suggests that the bio-concrete embedded with granular sludge cultivated using wastewater is highly corrosion-resistant than the ordinary concrete. This is likely attributed to the sulfur cycle between the aerobic and anaerobic layers of corrosion biofilms, which significantly reduces the biological sulfide uptake and the net production of acid. In contrast to current strategies for corrosion control, the granular sludge-based bio-concrete requires minimal maintenance and chemical admixtures. Considering the service life of sewers being up to 100 years, future research should focus on the long-term effectiveness of the bio-concrete, and the dynamics of SRB and SOB layers during the corrosion development. To enhance the viability of SRB, the addition

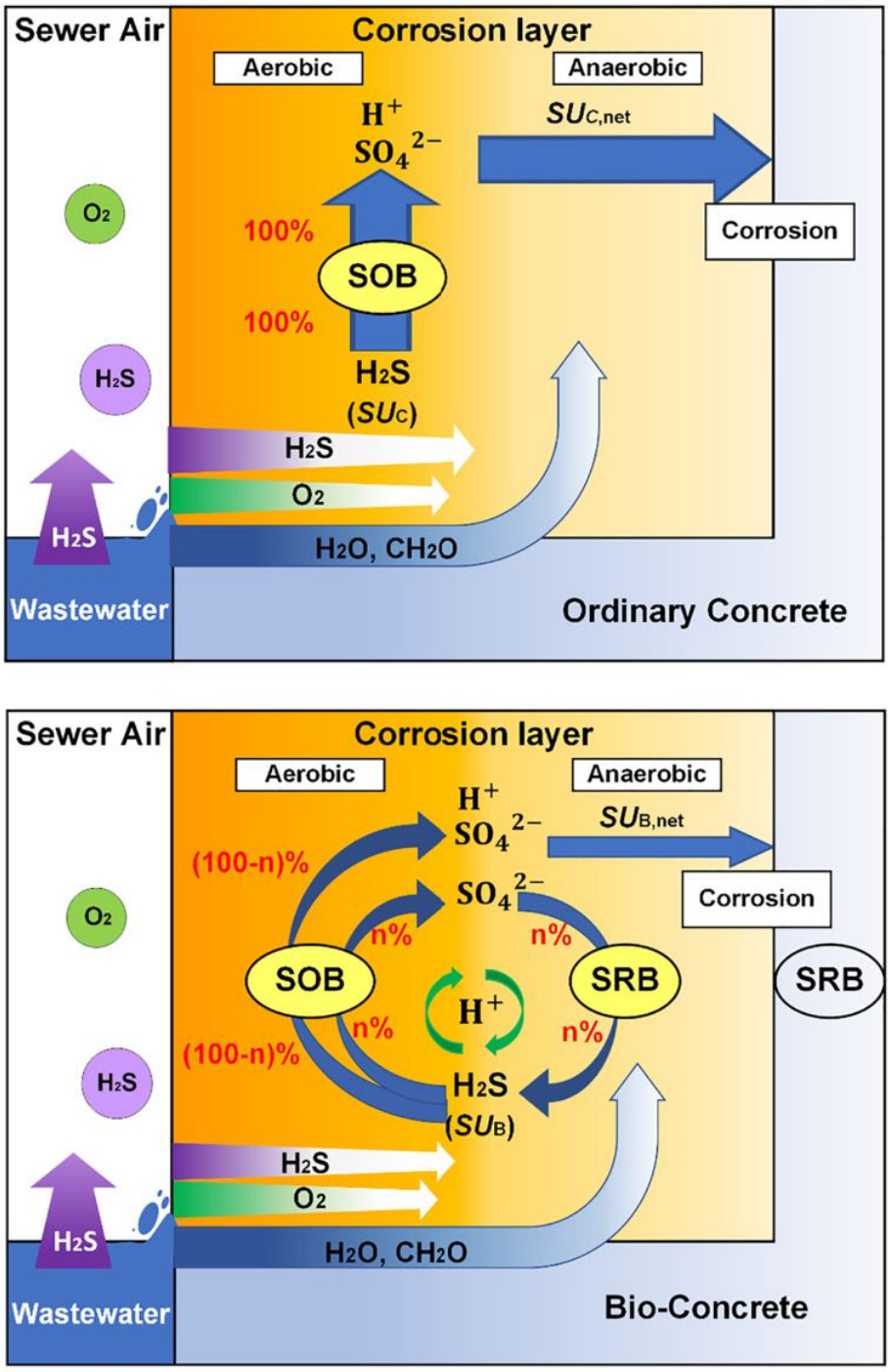

Fig. 5. A conceptual model for the corrosion-resistance of bio-concrete compared to ordinary concrete. CH_2O, the organic matters in wastewater. SU_C and SU_B, the total biological sulfide uptake by ordinary and bio-concrete; $SU_{C,\ net}$ and $SU_{B,\ net}$, the net sulfuric acid that caused corrosion in ordinary concrete and bio-concrete. In bio-concrete, n% represented the ratio of sulfide uptake kept in the sulfur cycle; (100-n)% represented the ratio of net sulfuric acid that causes corrosion. This model was mainly based on the co-existence of aerobic SOB and anaerobic SRB, and the cycling of sulfur between them in the corrosion layer.

of extra organic matters and higher SRB levels accumulated in the sludge would be beneficial. To reduce the impacts of granular sludge on the strength and porosity, investigations are needed to optimize the mix design.

4. Conclusions

The corrosion-resistance of a novel granular sludge-based bio-concrete, which was produced by mixing granular sludge enriched with indigenous wastewater bacteria into general concrete, was investigated by analyzing the physicochemical characteristics, corrosion products and microbial community. This has led to the following key findings:

- The addition of granular sludge significantly reduced concrete sewer corrosion. The corrosion rates of 1% and 2% bio-concrete were about 17.2% and 42.8% less than that of the control concrete, together with 14.6% and 35.0% less sulfide uptake rates, 15.3% and 55.6% less sulfate concentrations, and higher surface pH (up to 1.8 units).

- The major corrosion products for both bio-concrete and control concrete were gypsum and ettringite. However, the bio-concrete corrosion crystals were larger but less uniform than that of control concrete. The microstructure of corrosion products, for the first time, was utilized to delineate the corrosion development.
- The total relative abundance of SOB was significantly reduced on bio-concrete, while that of SRB was significantly enhanced compared to the control concrete. The corrosion-resistance of bio-concrete was mainly attributed to activities of SRB derived from the granular sludge, which supported the sulfur cycle between the aerobic and anaerobic corrosion sub-layers. The novel granular sludge-based bio-concrete provides a highly potential solution to reduce sewer corrosion.

CRediT authorship contribution statement

Yarong Song: Writing - original draft, Writing – review & editing, Conceptualization, Methodology, Investigation. **Kirthi Chetty:** Methodology. **Ulf Garbe:** Methodology. **Jing Wei:** Investigation. **Hao Bu:** Methodology. **Liza O'moore:** Resources. **Xuan Li:** Writing – review & editing. **Zhiguo Yuan:** Supervision, Writing – review & editing. **Timothy McCarthy:** Writing – review & editing. **Guangming Jiang:** Conceptualization, Writing – review & editing, Supervision, Funding acquisition.

Declaration of competing interest

The authors declare that they have no known competing financial interests or personal relationships that could have appeared to influence the work reported in this paper.

Acknowledgments

The authors acknowledge the financial support provided by Dr. Guangming Jiang's Australian Research Council DECRA Fellowship (DE170100694) and the Australian Research Council through Linkage Project LP150101337. Yarong is a recipient of the Early Career Researcher Philanthropic Grant 2020 at The University of Queensland. Dr. Xuan Li is supported by the ARC Discovery project (DP190100385). We also acknowledge the contribution from Dr. Elaine Wightman of Julius Kruttschnitt Mineral Research Centre and Ms. Ying Yu of Centre for Microscopy and Microanalysis at The University of Queensland.

Appendix A. Supplementary data

This Supplementary Information contains additional information about the properties of the synthetic and real wastewater, cultivation of granular sludge, concrete mix design and properties, corrosion chamber construction and operation, photogrammetry and mineral liberation analysis, sequencing data processing, and the rarefaction, rank abundance and principal component analysis using the sequencing results.

References

Achal, V., Mukerjee, A., Reddy, M.S., 2013. Biogenic treatment improves the durability and remediates the cracks of concrete structures. Constr. Build. Mater. 48, 1–5.

AS1012.21, 1999. Methods of testing concrete, method 21: determination of water absorption and apparent permeable voids in hardened concrete. AS1012.21, Standards Australian Sydney.

AS1012.9, 2014. Methods of testing concrete: Compressive strength tests-concrete, mortar and grout specimens. Standards Australia Sydney.

AS3972, 2010. General Purpose and Blended Cements. Standard, Standard Australia.

Berndt, M., 2011. Evaluation of coatings, mortars and mix design for protection of concrete against sulphur oxidising bacteria. Constr. Build. Mater. 25 (10), 3893–3902.

Boulos, P.F., Walker, A.T., 2015. Fixing the future of wastewater systems with smart water network modeling. J. Am. Water Works Assoc. 107 (4), 72–80.

Cayford, B.I., Dennis, P.G., Keller, J., Tyson, G.W., Bond, P.L., 2012. High-throughput amplicon sequencing reveals distinct communities within a corroding concrete sewer system. Appl. Environ. Microbiol. 78 (19), 7160–7162.

Cayford, B.I., Jiang, G., Keller, J., Tyson, G., Bond, P.L., 2017. Comparison of microbial communities across sections of a corroding sewer pipe and the effects of wastewater flooding. Biofouling 33 (9), 780–792.

Chahal, N., Rajor, A., Siddique, R., 2011. Calcium carbonate precipitation by different bacterial strains. Afr. J. Biotechnol. 10 (42), 8359–8372.

Chen, X., Wu, S., Zhou, J., 2013. Influence of porosity on compressive and tensile strength of cement mortar. Constr. Build. Mater. 40, 869–874.

Choi, Y., Naidu, G., Jeong, S., Lee, S., Vigneswaran, S., 2018. Effect of chemical and physical factors on the crystallization of calcium sulfate in seawater reverse osmosis brine. Desalination 426, 78–87.

Da Silva, F.B., De Belie, N., Boon, N., Verstraete, W., 2015. Production of non-axenic ureolytic spores for self-healing concrete applications. Constr. Build. Mater. 93, 1034–1041.

Davis, J.L., Nica, D., Shields, K., Roberts, D.J., 1998. Analysis of concrete from corroded sewer pipe. Int. Biodeterior. Biodegradation 42 (1), 75–84.

De Muynck, W., De Belie, N., Verstraete, W., 2009. Effectiveness of admixtures, surface treatments and antimicrobial compounds against biogenic sulfuric acid corrosion of concrete. Cem. Concr. Compos. 31 (3), 163–170.

Dickson, A., Millero, F.J., 1987. A comparison of the equilibrium constants for the dissociation of carbonic acid in seawater media. Deep Sea Research Part A. Oceanographic Research Papers. 34, (10), pp. 1733–1743.

Dopson, M., Baker-Austin, C., Hind, A., Bowman, J.P., Bond, P.L., 2004. Characterization of Ferroplasma isolates and Ferroplasma acidarmanus sp. nov., extreme acidophiles from acid mine drainage and industrial bioleaching environments. Appl. Environ. Microbiol. 70 (4), 2079–2088.

EPA, U., 1991. Hydrogen Sulphide Corrosion in Wastewater Collection and Treatment System.

Erşan, Y.Ç., Gruyaert, E., Louis, G., Lors, C., De Belie, N., Boon, N., 2015a. Self-protected nitrate reducing culture for intrinsic repair of concrete cracks. Front. Microbiol. 6, 1228.

Erşan, Y.Ç., Da Silva, F.B., Boon, N., Verstraete, W., De Belie, N., 2015b. Screening of bacteria and concrete compatible protection materials. Constr. Build. Mater. 88, 196–203.

Erşan, Y.Ç., Hernandez-Sanabria, E., Boon, N., De Belie, N., 2016. Enhanced crack closure performance of microbial mortar through nitrate reduction. Cem. Concr. Compos. 70, 159–170.

Fandrich, R., Gu, Y., Burrows, D., Moeller, K., 2007. Modern SEM-based mineral liberation analysis. Int. J. Miner. Process. 84 (1), 310–320.

Ganigue, R., Gutierrez, O., Rootsey, R., Yuan, Z., 2011. Chemical dosing for sulfide control in Australia: an industry survey. Water Res. 45 (19), 6564–6574.

Garbe, U., Randall, T., Hughes, C., Davidson, G., Pangelis, S., Kennedy, S., 2015. A new neutron radiography/tomography/imaging station DINGO at OPAL. Phys. Procedia 69, 27–32.

Grengg, C., Mittermayr, F., Ukrainczyk, N., Koraimann, G., Kienesberger, S., Dietzel, M., 2018a. Advances in concrete materials for sewer systems affected by microbial induced concrete corrosion: a review. Water Res. 134, 341–352.

Grengg, C., Mittermayr, F., Ukrainczyk, N., Koenders, E., Koraimann, G., Kienesberger, S., Dietzel, M., 2018b. Microbial induced acid corrosion from a field perspective-Advances in process understanding and construction material development. MATEC Web of Conferences, 2018; EDP Sciences, p. 02002.

Grengg, C., Ukrainczyk, N., Koraimann, G., Mueller, B., Dietzel, M., Mittermayr, F., 2020. Long-term in situ performance of geopolymer, calcium aluminate and Portland cement-based materials exposed to microbially induced acid corrosion. Cem. Concr. Res. 131, 106034.

Haile, T., Nakhla, G., 2010. The inhibitory effect of antimicrobial zeolite on the biofilm of Acidithiobacillus thiooxidans. Biodegradation 21 (1), 123.

Hammes, F., Verstraete, W., 2002. Key roles of pH and calcium metabolism in microbial carbonate precipitation. Rev. Environ. Sci. Biotechnol. 1 (1), 3–7.

Hvitved-Jacobsen, T., Vollertsen, J., Nielsen, A.H., 2013. Sewer Processes: Microbial and Chemical Process Engineering of Sewer Networks. CRC press.

Islander, R.L., Devinny, J.S., Mansfeld, F., Postyn, A., Shih, H., 1991. Microbial ecology of crown corrosion in sewers. J. Environ. Eng. 117 (6), 751–770.

Jahani, F., Devinny, J., Mansfeld, F., Rosen, I., Sun, Z., Wang, C., 2001. Investigations of sulfuric acid corrosion of concrete. I: modeling and chemical observations. J. Environ. Eng. 127 (7), 572–579.

Jiang, G., Sharma, K.R., Guisasola, A., Keller, J., Yuan, Z., 2009. Sulfur transformation in rising main sewers receiving nitrate dosage. Water Res. 43 (17), 4430–4440.

Jiang, G., Keller, J., Bond, P.L., 2014a. Determining the long-term effects of H 2 S concentration, relative humidity and air temperature on concrete sewer corrosion. Water Res. 65, 157–169.

Jiang, G., Wightman, E., Donose, B.C., Yuan, Z., Bond, P.L., Keller, J., 2014b. The role of iron in sulfide induced corrosion of sewer concrete. Water Res. 49, 166–174.

Jiang, G., Sun, X., Keller, J., Bond, P.L., 2015. Identification of controlling factors for the initiation of corrosion of fresh concrete sewers. Water Res. 80, 30–40.

Jiang, G., Zhou, M., Chiu, T.H., Sun, X., Keller, J., Bond, P.L., 2016. Wastewater-enhanced microbial corrosion of concrete sewers. Environ. Sci. Technol. 50 (15), 8084–8092.

Jiang, G., Melder, D., Keller, J., Yuan, Z., 2017. Odor emissions from domestic wastewater: a review. Crit. Rev. Environ. Sci. Technol. 47 (17), 1581–1611.

Joseph, A.P., Keller, J., Bustamante, H., Bond, P.L., 2012. Surface neutralization and H 2 S oxidation at early stages of sewer corrosion: influence of temperature, relative humidity and H 2 S concentration. Water Res. 46 (13), 4235–4245.

Koch, G.H., Brongers, M.P., Thompson, N.G., Virmani, Y.P., Payer, J.H., 2002. Corrosion Cost and Preventive Strategies in the United States.

Lai, C.-Y., Dong, Q.-Y., Rittmann, B.E., Zhao, H.-P., 2018a. Bioreduction of antimonate by anaerobic methane oxidation in a membrane biofilm batch reactor. Environ. Sci. Technol. 52 (15), 8693–8700.

Lai, C.-Y., Dong, Q.-Y., Chen, J.-X., Zhu, Q.-S., Yang, X., Chen, W.-D., Zhao, H.-P., Zhu, L., 2018b. Role of extracellular polymeric substances in a methane based membrane biofilm reactor reducing vanadate. Environ. Sci. Technol. 52 (18), 10680–10688.
Lebrero, R., Bouchy, L., Stuetz, R., Muñoz, R., 2011. Odor assessment and management in wastewater treatment plants: a review. Crit. Rev. Environ. Sci. Technol. 41 (10), 915–950.
Li, X., Kappler, U., Jiang, G., Bond, P.L., 2017. The ecology of acidophilic microorganisms in the corroding concrete sewer environment. Front. Microbiol. 8.
Li, X., Bond, P.L., O'Moore, L., Wilkie, S., Hanzic, L., Johnson, I., Mueller, K., Yuan, Z., Jiang, G., 2020a. Increased resistance of nitrite-admixed concrete to microbially induced corrosion in real sewers. Environ. Sci. Technol. 54 (4), 2323–2333.
Li, X., O'Moore, L., Wilkie, S., Song, Y., Wei, J., Bond, P.L., Yuan, Z., Hanzic, L., Jiang, G., 2020b. Nitrite admixed concrete for wastewater structures: mechanical properties, leaching behavior and biofilm development. Constr. Build. Mater. 233, 117341.
Ling, A.L., 2013. Characterization and Control of Microbially Induced Concrete Corrosion. University of Colorado at Boulder.
Ling, A.L., Robertson, C.E., Harris, J.K., Frank, D.N., Kotter, C.V., Stevens, M.J., Pace, N.R., Hernandez, M.T., 2014. Carbon dioxide and hydrogen sulfide associations with regional bacterial diversity patterns in microbially induced concrete corrosion. Environ. Sci. Technol. 48 (13), 7357–7364.
Ma, C., Chen, B., Chen, L., 2016. Effect of organic matter on strength development of self-compacting earth-based construction stabilized with cement-based composites. Constr. Build. Mater. 123, 414–423.
Monteny, J., Vincke, E., Beeldens, A., De Belie, N., Taerwe, L., Van Gemert, D., Verstraete, W., 2000. Chemical, microbiological, and in situ test methods for biogenic sulfuric acid corrosion of concrete. Cem. Concr. Res. 30 (4), 623–634.
Mori, T., Nonaka, T., Tazaki, K., Koga, M., Hikosaka, Y., Noda, S., 1992. Interactions of nutrients, moisture and pH on microbial corrosion of concrete sewer pipes. Water Res. 26 (1), 29–37.
Negishi, A., Muraoka, T., Maeda, T., Takeuchi, F., Kanao, T., Kamimura, K., Sugio, T., 2005. Growth inhibition by tungsten in the sulfur-oxidizing bacterium Acidithiobacillus thiooxidans. Biosci. Biotechnol. Biochem. 69 (11), 2073–2080.
Ni, G., Simone, D., Palma, D., Broman, E., Wu, X., Turner, S., Dopson, M., 2018. A novel inorganic sulfur compound metabolizing Ferroplasma-like population is suggested to mediate extracellular electron transfer. Front. Microbiol. 9, 2945.
Nielsen, A.H., Hvitved-Jacobsen, T., Vollertsen, J., 2012. Effect of sewer headspace air-flow on hydrogen sulfide removal by corroding concrete surfaces. Water Environ. Res. 84 (3), 265–273.
Okabe, S., Itoh, T., Satoh, H., Watanabe, Y., 1999. Analyses of spatial distributions of sulfate-reducing bacteria and their activity in aerobic wastewater biofilms. Appl. Environ. Microbiol. 65 (11), 5107–5116.
Okabe, S., Ito, T., Sugita, K., Satoh, H., 2005. Succession of internal sulfur cycles and sulfur-oxidizing bacterial communities in microaerophilic wastewater biofilms. Appl. Environ. Microbiol. 71 (5), 2520–2529.
Okabe, S., Odagiri, M., Ito, T., Satoh, H., 2007. Succession of sulfur-oxidizing bacteria in the microbial community on corroding concrete in sewer systems. Appl. Environ. Microbiol. 73 (3), 971–980.
Oromiehie, E., Garbe, U., Gangadhara Prusty, B., 2020. Porosity analysis of carbon fibre-reinforced polymer laminates manufactured using automated fibre placement. J. Compos. Mater. 54 (9), 1217–1231.
Parande, A., Ramsamy, P., Ethirajan, S., Rao, C., Palanisamy, N., 2006. Deterioration of reinforced concrete in sewer environments. Proceedings of the Institution of Civil Engineers-Municipal Engineer, 2006. Thomas Telford Ltd, pp. 11–20.
Parker, C., 1945a. The corrosion of concrete 1. The isolation of a species of bacterium associated with the corrosion of concrete exposed to atmospheres containing hydrogen sulphide. Aust. J. Exp. Biol. Med. Sci. 23, 2.
Parker, C., 1945b. The corrosion of concrete 2. The function of Thiobacillus concretivorus (nov. spec.) in the corrosion of concrete exposed to atmospheres containing hydrogen sulphide. Aust. J. Exp. Biol. Med. Sci. 23, 2.
Pikaar, I., Sharma, K.R., Hu, S., Gernjak, W., Keller, J., Yuan, Z., 2014. Reducing sewer corrosion through integrated urban water management. Science 345 (6198), 812–814.
Saraswathy, V., Song, H.-W., 2007. Improving the durability of concrete by using inhibitors. Build. Environ. 42 (1), 464–472.
Satoh, H., Odagiri, M., Ito, T., Okabe, S., 2009. Microbial community structures and in situ sulfate-reducing and sulfur-oxidizing activities in biofilms developed on mortar specimens in a corroded sewer system. Water Res. 43 (18), 4729–4739.
Seifan, M., Samani, A.K., Berenjian, A., 2016. Bioconcrete: next generation of self-healing concrete. Appl. Microbiol. Biotechnol. 100 (6), 2591–2602.
Silva, F.B., Boon, N., De Belie, N., Verstraete, W., 2015. Industrial application of biological self-healing concrete: challenges and economical feasibility. J. Commer. Biotechnol. 21, 1.
Song, Y., Tian, Y., Li, X., Wei, J., Zhang, H., Bond, P.L., Yuan, Z., Jiang, G., 2019a. Distinct microbially induced concrete corrosion at the tidal region of reinforced concrete sewers. Water Res. 150, 392–402.
Song, Y., Wightman, E., Tian, Y., Jack, K., Li, X., Zhong, H., Bond, P.L., Yuan, Z., Jiang, G., 2019b. Corrosion of reinforcing steel in concrete sewers. Sci. Total Environ. 649, 739–748.
Song, Y., Wightman, E., Kulandaivelu, J., Bu, H., Wang, Z., Yuan, Z., Jiang, G., 2020. Rebar corrosion and its interaction with concrete degradation in reinforced concrete sewers. Water Res. 182, 115961.
Strigul, N., Koutsospyros, A., Christodoulatos, C., 2010. Tungsten speciation and toxicity: acute toxicity of mono-and poly-tungstates to fish. Ecotoxicol. Environ. Saf. 73 (2), 164–171.
Sun, X., Jiang, G., Bond, P.L., Wells, T., Keller, J., 2014. A rapid, non-destructive methodology to monitor activity of sulfide-induced corrosion of concrete based on H2S uptake rate. Water Res. 59, 229–238.
Sun, X., Jiang, G., Bond, P.L., Keller, J., Yuan, Z., 2015. A novel and simple treatment for control of sulfide induced sewer concrete corrosion using free nitrous acid. Water Res. 70, 279–287.
Sun, X., Jiang, G., Chiu, T.H., Zhou, M., Keller, J., Bond, P.L., 2016. Effects of surface washing on the mitigation of concrete corrosion under sewer conditions. Cem. Concr. Compos. 68, 88–95.
Vahidi, E., Jin, E., Das, M., Singh, M., Zhao, F., 2016. Environmental life cycle analysis of pipe materials for sewer systems. Sustain. Cities Soc. 27, 167–174.
Vollertsen, J., Nielsen, A.H., Jensen, H.S., Wium-Andersen, T., Hvitved-Jacobsen, T., 2008. Corrosion of concrete sewers—the kinetics of hydrogen sulfide oxidation. Sci. Total Environ. 394 (1), 162–170.
Wang, J., Van Tittelboom, K., De Belie, N., Verstraete, W., 2012a. Use of silica gel or polyurethane immobilized bacteria for self-healing concrete. Constr. Build. Mater. 26 (1), 532–540.
Wang, B., Sivret, E.C., Parcsi, G., Wang, X., Stuetz, R.M., 2012b. Characterising volatile organic compounds from sewer emissions by thermal desorption coupled with gas-chromatography-mass spectrometry. Chem. Eng. 30, 73–78.
Wells, T., Melchers, R., 2014. An observation-based model for corrosion of concrete sewers under aggressive conditions. Cem. Concr. Res. 61, 1–10.
Wells, T., Melchers, R., 2015. Modelling concrete deterioration in sewers using theory and field observations. Cem. Concr. Res. 77, 82–96.
Wells, T., Melchers, R.E., Bond, P., 2009. Factors involved in the long term corrosion of concrete sewers. Australasian Corrosion Association Proceedings of Corrosion and Prevention, Coffs Harbour, Australia, p. 11.
Zhao, Y., Yu, J., Hu, B., Jin, W., 2012. Crack shape and rust distribution in corrosion-induced cracking concrete. Corros. Sci. 55, 385–393.
Zhu, T., Dittrich, M., 2016. Carbonate precipitation through microbial activities in natural environment, and their potential in biotechnology: a review. Front. Bioeng. Biotechnol. 4, 4.